Supplementary material for the manuscript titled "The Eocene-Oligocene Transition in the Paratethys: Boreal Water Ingression and its Paleoceanographic Implications"

Mustafa Yücel Kaya[1], Henk Brinkhuis[2, 3], Chiara Fioroni[4], Serdar Görkem Atasoy[1], Alexis Licht[5], Dirk Nürnberg[6], Taylan Vural[1]

[1]Department of Geological Engineering, Middle East Technical University, Ankara, 06800, Türkiye

[2]Oceans Systems research (OCS), NIOZ Royal Netherlands Institute of Sea Research, Texel, 1790 AB The Netherlands

[3]Earth Sciences dept., Laboratory of Palaeobotany and Palynology, Faculty of Geosciences, Utrecht University, 3584 CB Utrecht, The Netherlands

[4]Dipartimento di Scienze Chimiche e Geologiche, Università degli Studi di Modena e Reggio Emilia, Modena, 41121, Italy.

[5]Aix-Marseille Université, CNRS, IRD, INRAE, Collège de France, CEREGE, Technopôle de l'Arbois-Méditerranée, BP80, 13545 Aix-en-Provence, France

[6]GEOMAR Helmholtz Centre for Ocean Research Kiel, Kiel, D-24148, Germany

Supplementary Figures & Tables

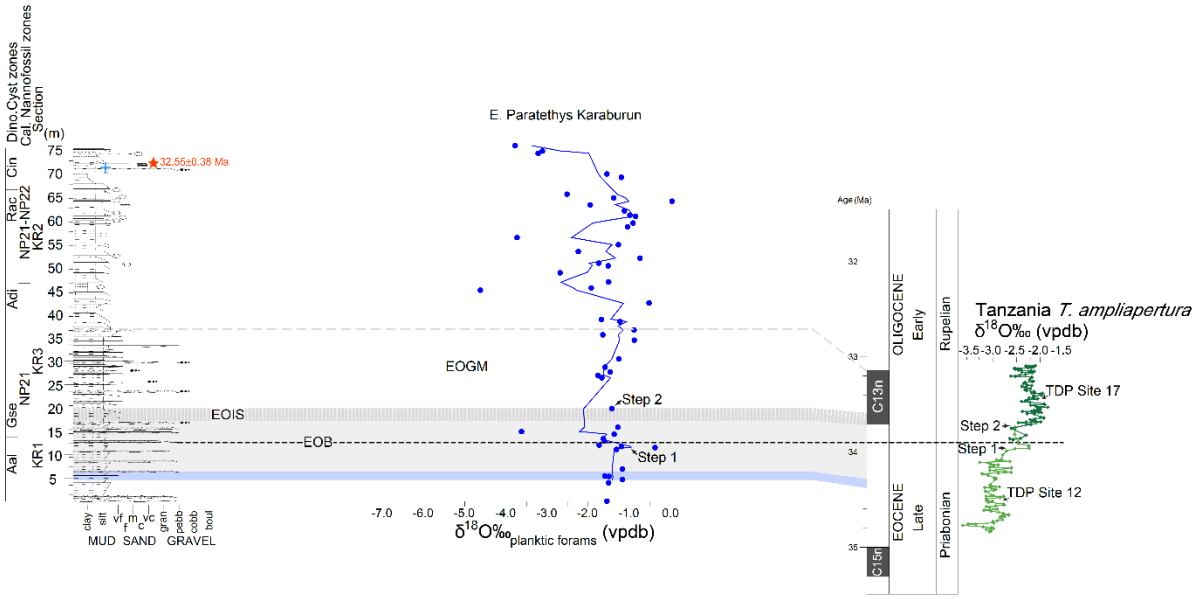

Figure S1 The stratigraphic log (in meters) of the Karaburun composite section including the results of planktic foraminifera δ¹⁸O record (blue dots and line showing three-point running mean), highlighting the chronostratigraphic characteristics of the Eocene-Oligocene Transition (EOT, light gray shading). Apparent correlations were established by aligning the Karaburun data with high-resolution planktic foraminifera δ¹⁸O records from the the African margin of the Indian Ocean (Tanzania Drilling Project sites 12 and 17, Pearson et al., 2008). Key features in the δ¹⁸O records, such as positive and negative shifts and their amplitudes, were used to establish correlations. The EOT characteristics, including the Late Eocene Event (light blue shading), the Earliest Oligocene Oxygen Isotope Step (EOIS) and the Early Oligocene Glacial Maximum (EOGM) were defined by the δ¹⁸O benthic foraminifera record (see Figure 3 in the main manuscript). The Eocene-Oligocene Boundary (EOB) was identified through biostratigraphic analyses (see section 5.1 in the main manuscript). The red star on the log marks the tuff layer, while the blue cross indicates the occurrence of the cold-water dinocyst *Svalbardella cooksoniae*.

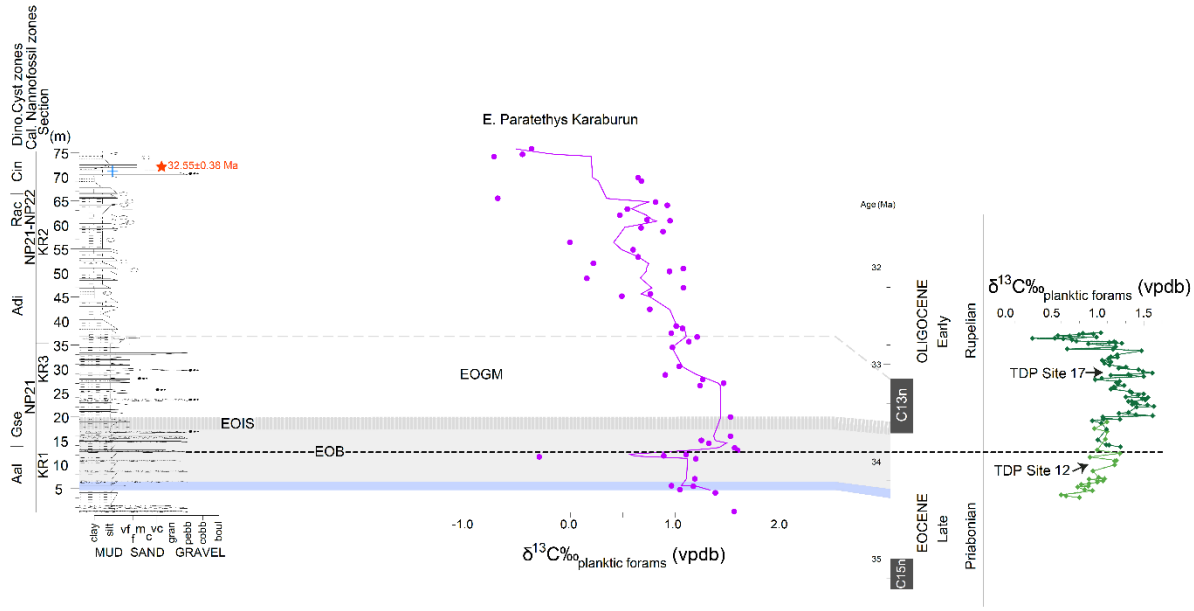

Figure S2 The stratigraphic log (in meters) of the Karaburun composite section including the results of planktic foraminifera $\delta^{13}C$ record (purple dots and line showing three-point running mean), highlighting the chronostratigraphic characteristics of the Eocene-Oligocene Transition (EOT, light gray shading). Apparent correlations were established by aligning the Karaburun data with high-resolution planktic foraminifera $\delta^{13}C$ records from the the African margin of the Indian Ocean (Tanzania Drilling Project sites 12 and 17, Pearson et al., 2008). Key features in the $\delta^{18}O$ records, such as positive and negative shifts and their amplitudes, were used to establish correlations. The EOT characteristics, including the Late Eocene Event (light blue shading), the Earliest Oligocene Oxygen Isotope Step (EOIS) and the Early Oligocene Glacial Maximum (EOGM) were defined by the $\delta^{18}O$ benthic foraminifera record (see Figure 3 in the main manuscript). The Eocene-Oligocene Boundary (EOB) was identified through biostratigraphic analyses (see section 5.1 in the main manuscript). The red star on the log marks the tuff layer, while the blue cross indicates the occurrence of the cold-water dinocyst *Svalbardella cooksoniae*.

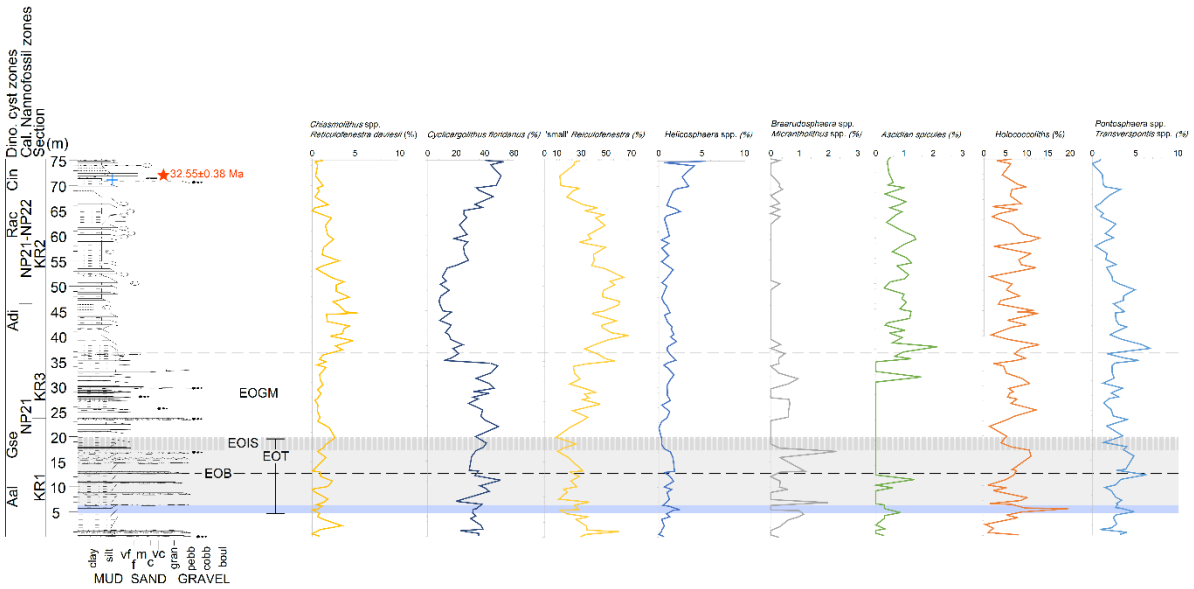

Figure S3 The stratigraphic log (in meters) of the Karaburun composite section including relative abundances (%) of calcareous nannofossil assemblages which are indicative of paleoenvironmental conditions (see section 5.5.1 in the main manuscript). The EOT characteristics, including the Late Eocene Event (light blue shading), the Earliest Oligocene Oxygen Isotope Step (EOIS) and the Early Oligocene Glacial Maximum (EOGM) were defined by the $\delta^{18}O$ benthic foraminifera record (see Figure 3 in the main manuscript). The Eocene-Oligocene Boundary (EOB) was identified through biostratigraphic analyses (see section 5.1 in the main manuscript). The red star on the log marks the tuff layer, while the blue cross indicates the occurrence of the cold-water dinocyst *Svalbardella cooksoniae*.

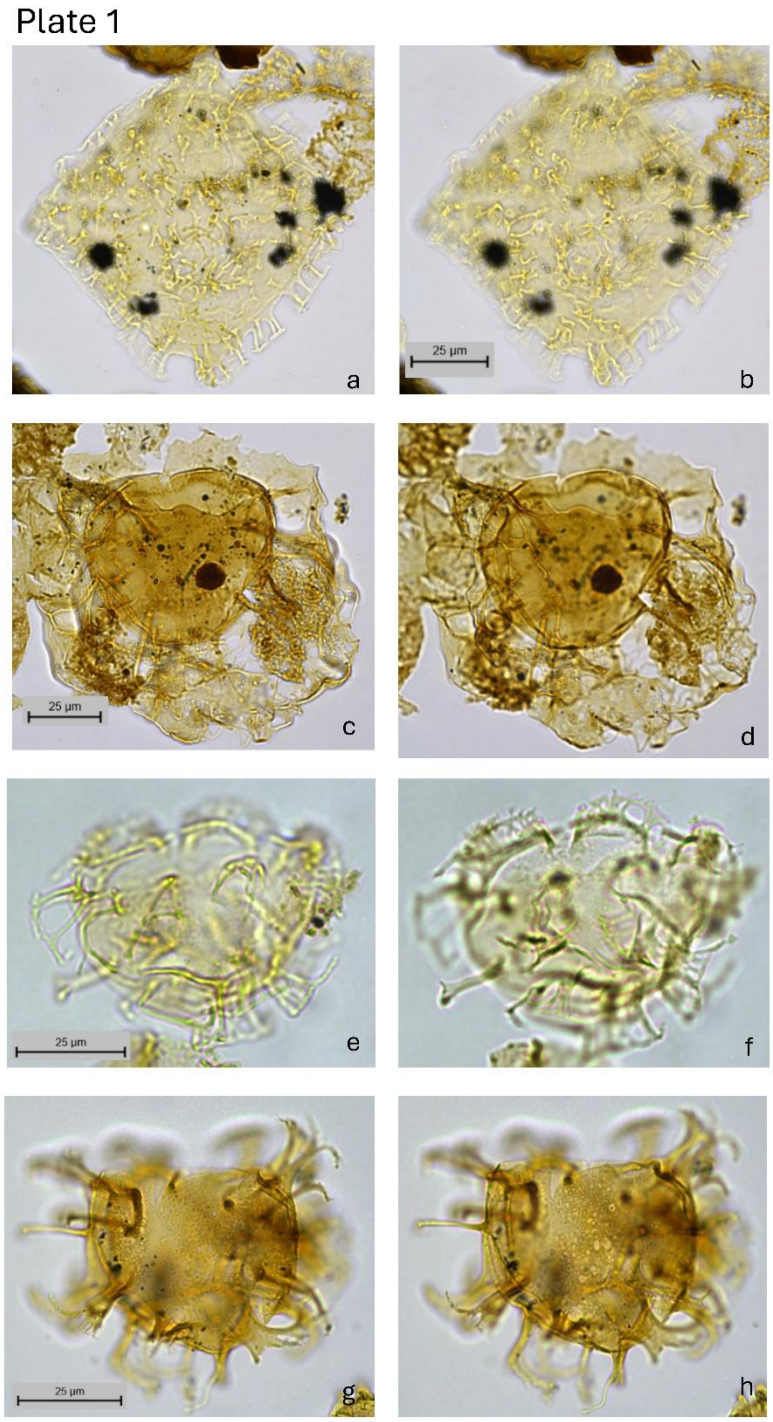

Figure S4 Plate 1 microphotographs of selected dinocyst taxa from the Karaburun sections

a, b. *Charlesdowniea clathrata.* Sample KR22S2Y32, slide 1, EF: C41. a: dorsal view. b. internal ventral view.

c, d. *Glaphyrocysta semitecta.* Sample KR22S2Y14, slide 1, EF: V24-1. c: ventral view. d. internal dorsal view.

e, f. *Hemiplacophora semilunifera*. Sample KR22S1Y1, slide 2. EF: T42-4. e: ventral view. f. internal dorsal view.

g, h. *Licracysta semicirculata*. Sample KR22S2Y45, slide 1. EF: R43-2. g: dorsal view. h. internal ventral view.

114

Plate 2

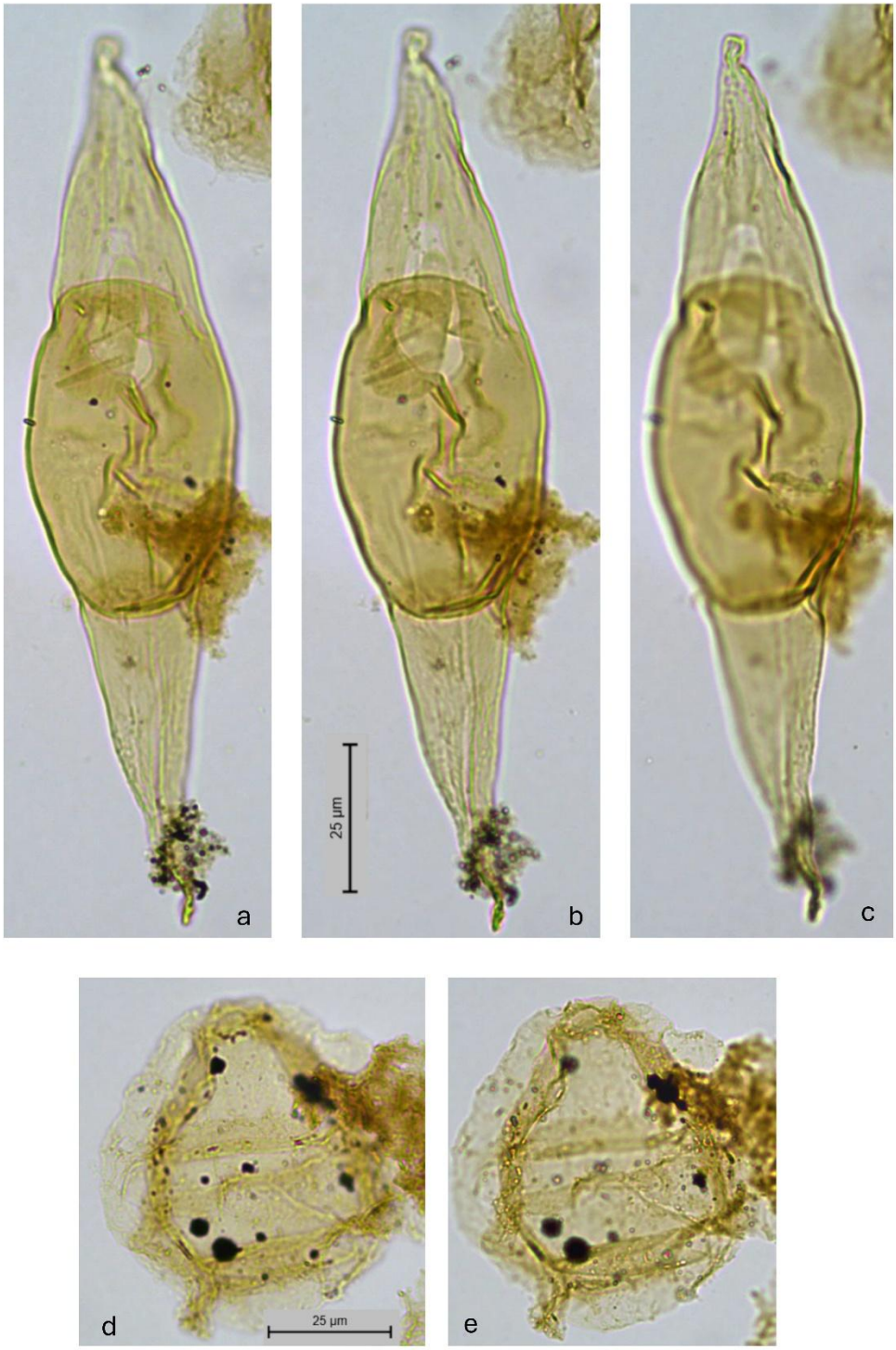

115

116 **Figure S5 Plate 2 microphotographs of selected dinocyst taxa from the Karaburun sections**

117 a, b, c. *Svalbardella cooksoniae.* Sample KR22S2Y41, slide 2, EF: G17-3. a: dorsal view. b. internal
118 view, mid focus. c: internal ventral view.

119 d, e. *Ascostomocystis potane*. Sample KR22S2Y8, slide 1. EF: E22-3. d. external view, upper focus. e.
120 internal view, low focus.

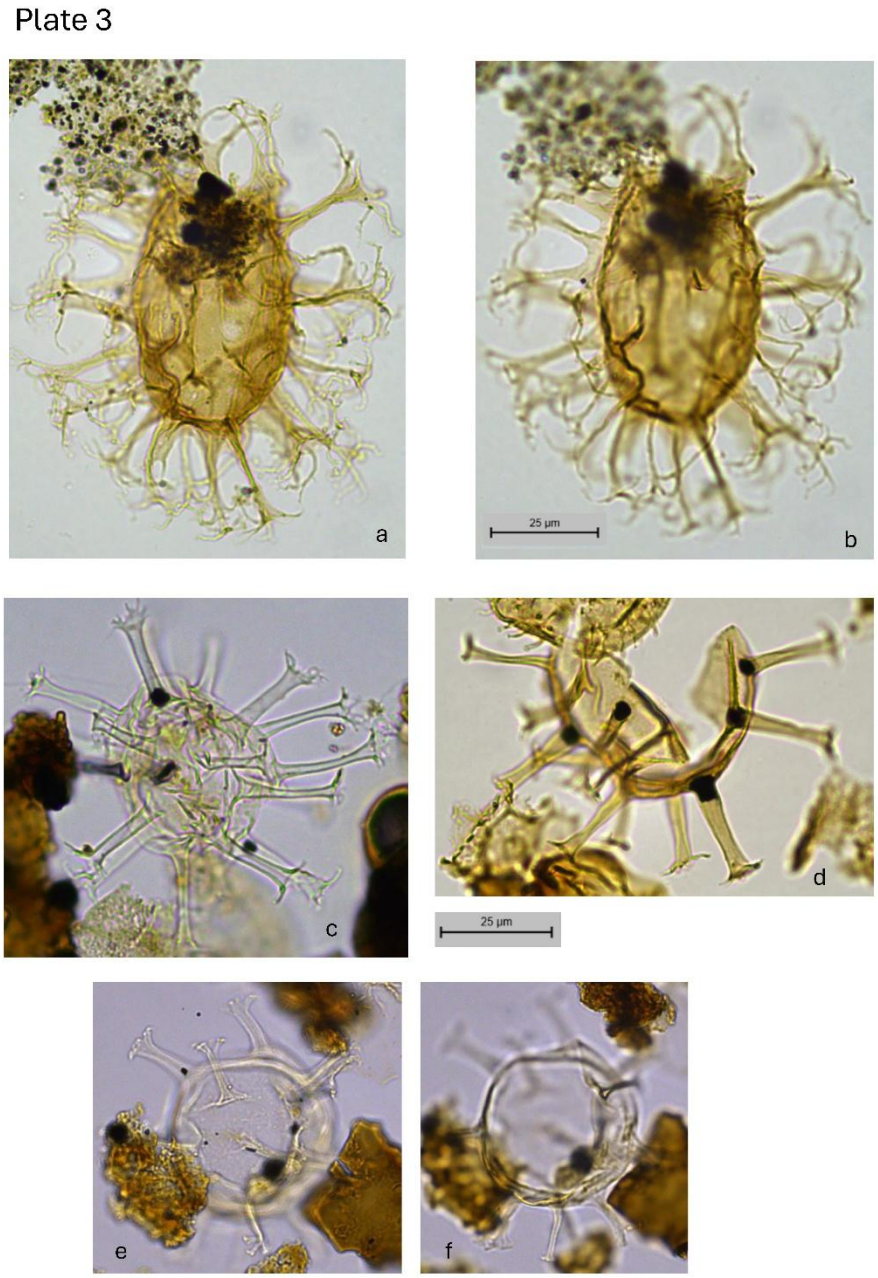

Figure S6 Plate 3 microphotographs of selected dinocyst taxa from the Karaburun sections

a, b. *Distatodinium ellipticum.* KR22S2Y45, slide 1, EF: M42. a: ventral view. b. internal dorsal view.

c. *Homotryblium pallidum*. Sample KR21Y3, slide 1, EF: M25.

d. *Homotryblium aculeatum*. Sample KR22S2Y1, slide 1, EF: D16-3.

e., f. *Homotryblium floripes*. Sample KR2Y31, slide 1, EF: U33-4.

Plate 4

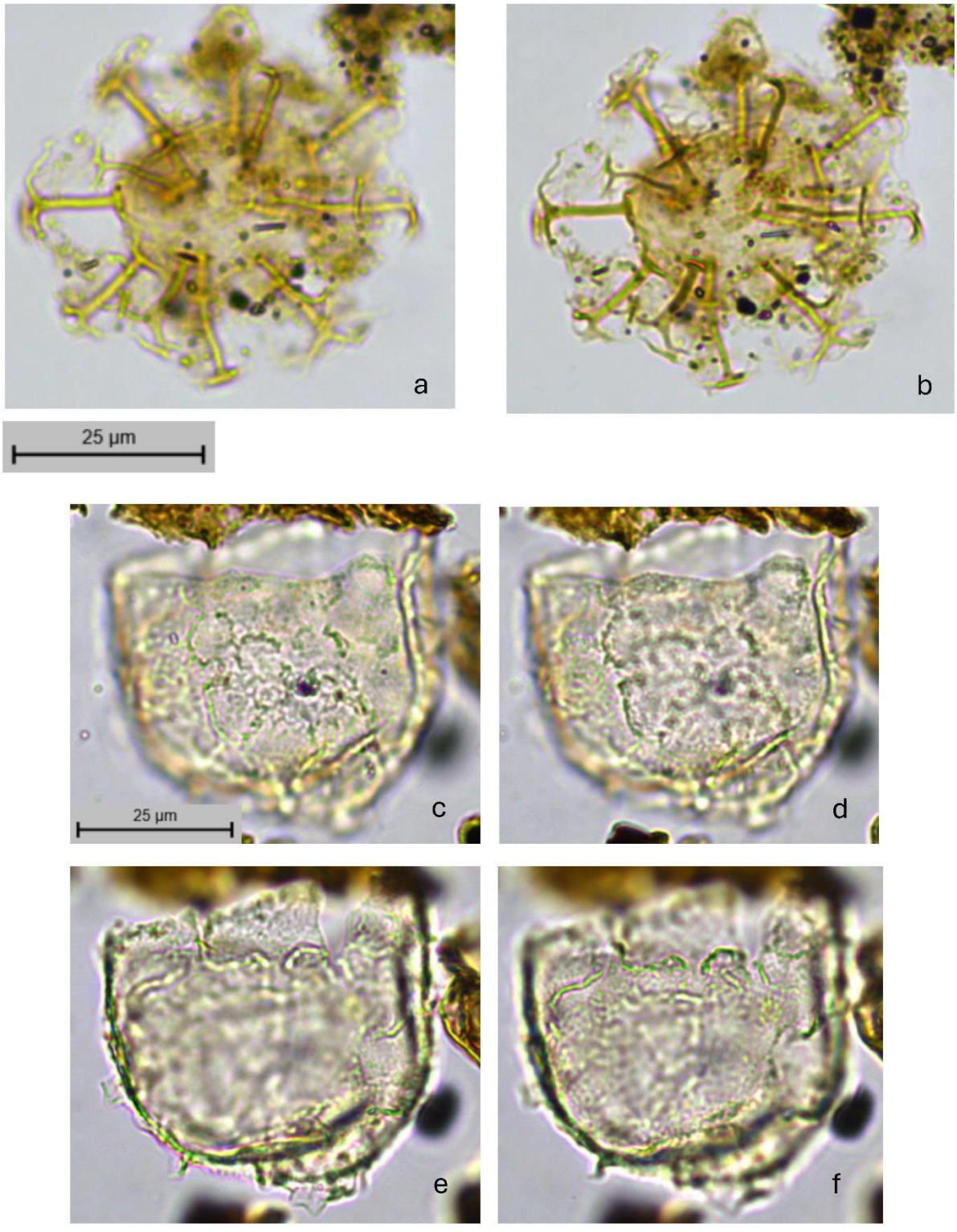

Figure S7 Plate 4 microphotographs of selected dinocyst taxa from the Karaburun sections

a, b. *Reticulatosphaera actinocoronata.* Sample KR22S2Y14, slide 1, EF: O41-1, orientation unknown.

c-f. *Stoveracysta* sp. 1 of Brinkhuis and Biffi 1993. Sample KR3Y15, slide 1, EF: O27-1. c. oblique dorsal view. d. mid focus level 1, e. mid focus level 2. f. oblique internal ventral view.

Plate 5

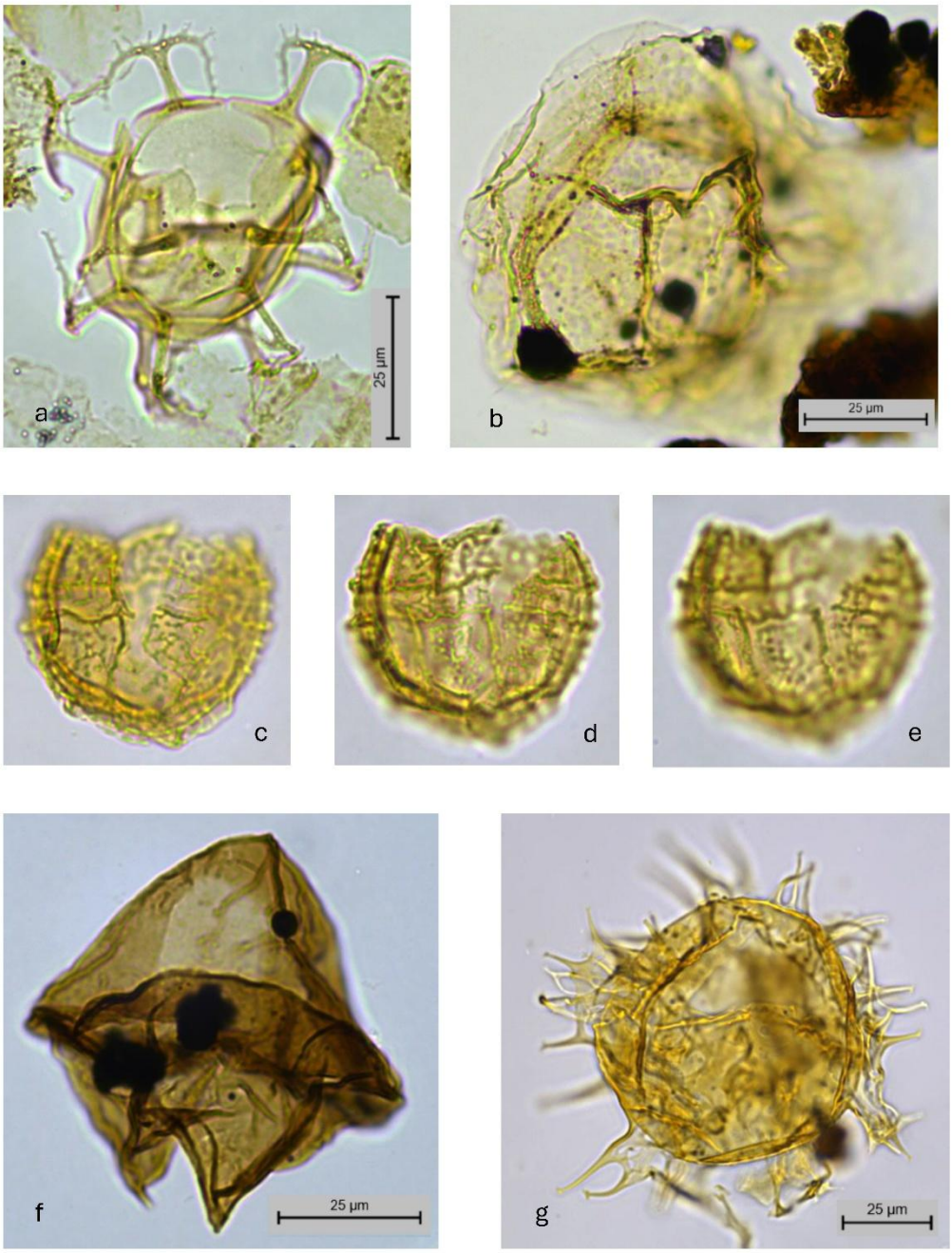

Figure S8 Plate 5 microphotographs of selected dinocyst taxa from the Karaburun sections

a. Enneadocysta pectiniforme. Sample KR22S1Y1, slide 1, EF: M42.

b. Heteraulacacysta porosa. Sample KR3Y30, slide 2, EF: R36

c-e. *Microdinium reticulatum.* Sample KR21Y3, slide 1, EF: M25. c: ventral view. d. internal view, mid focus. e: internal dorsal view.

f. *Lejeunecysta fallax* . Sample KR22S2Y1, slide 1, EF: D34. Oblique dorsal view.

g. *Glaphyrocysta priabonensis*. Sample KR22S1Y8, slide 1, EF: K42-2.

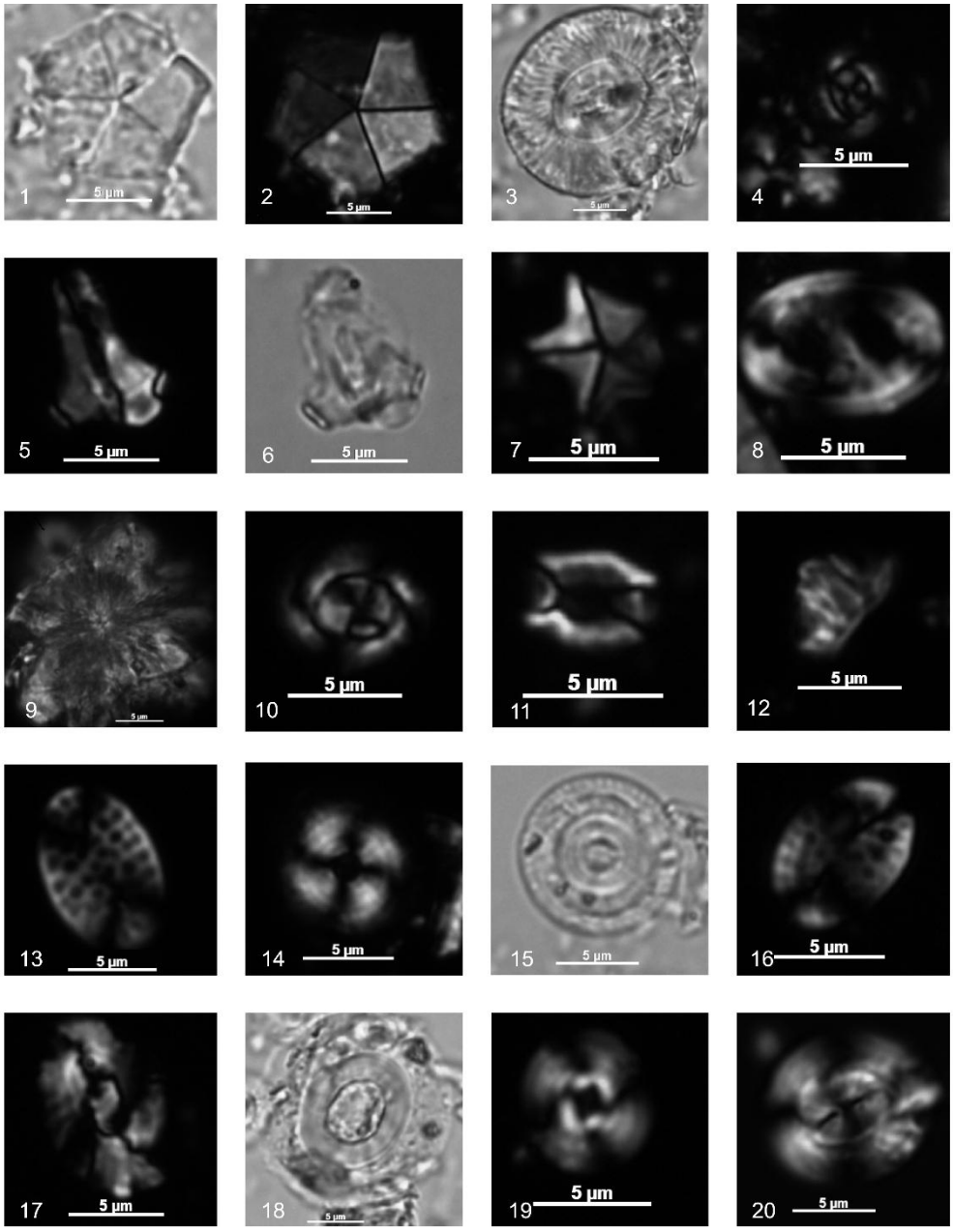

Figure S9 Plate 6 LM (magnification 1250x) microphotographs of selected calcareous nannofossil taxa from the Karaburun sections.

1. *Braarudosphaera bigelowii* . Sample KR3-Y14, parallel light. **2.** *Braarudosphaera bigelowii* . Sample KR3-Y14, crossed nicols. **3**. *Coccolithus eopelagicus*. Sample KR3-Y14, parallel light. **4.** *Clausicoccus subdistichus*, Sample KR3-Y14, crossed nicols. **5.** *Zigrablithus bijugatus*. Sample KR1-N12, crossed nicols . **6.** *Zigrablithus bijugatus*. Sample KR1-N12, parallel light. **7.** *Micrantholithus vesper*. Sample KR3-Y14, crossed nicols. **8.** *Pontosphaera pulcheroides*. Sample KR3-Y14, crossed nicols. **9**. *Ascidian spicules*. Sample KR1-N16, crossed nicols. **10.** *Clausicoccus fenestratus.* Sample KR2-N20, crossed nicols. **11**. *Lanternithus minutus.* Sample KR3-Y14, crossed nicols.**12**. *Orthozygus aureus*. Sample KR1-N16, crossed nicols. **13**. *Pontosphaera multipora*. Sample KR1-N16, crossed nicols. **14.** *Ericsonia formosa*. Sample KR1-N12, crossed nicols. **15**. *Ericsonia formosa*. Sample KR1-N12, parallel light. **16**. *Pontosphaera punctosa*. Sample KR2-N20, crossed nicols. **17.** *Helicosphaera euphratis.* Sample KR2-N20, crossed nicols.**18**. *Reticulofenestra umbilicus.* Sample KR1-N12, parallel light. **19.** *Cyclicargolithus floridanus*. Sample KR1-N12, crossed nicols. **20.** *Dictyococcites bisectus.* Sample KR2-N20, crossed nicols.

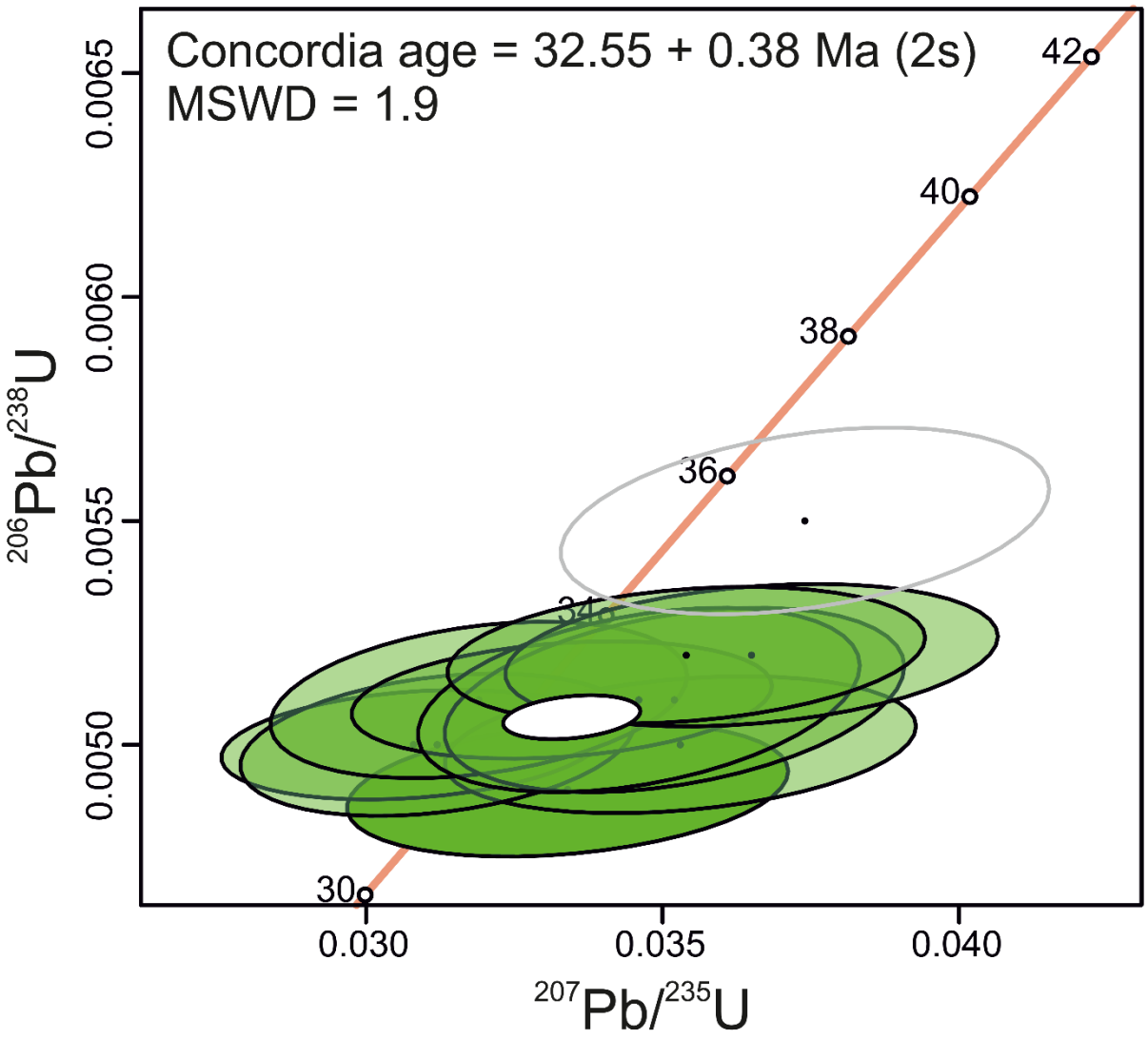

Figure S10 Pb/U Concordia diagram of the 12 single zircon grains screened as concordant, with their 2s uncertainty (green circles). The calculated Concordia age and its 2s uncertainty are also displayed. The outlier that is not included in the Concordia age calculation is shown with an empty circle. The plot and calculations were generated with IsoPlotR. MSWD: Mean Square Weighted Deviation.

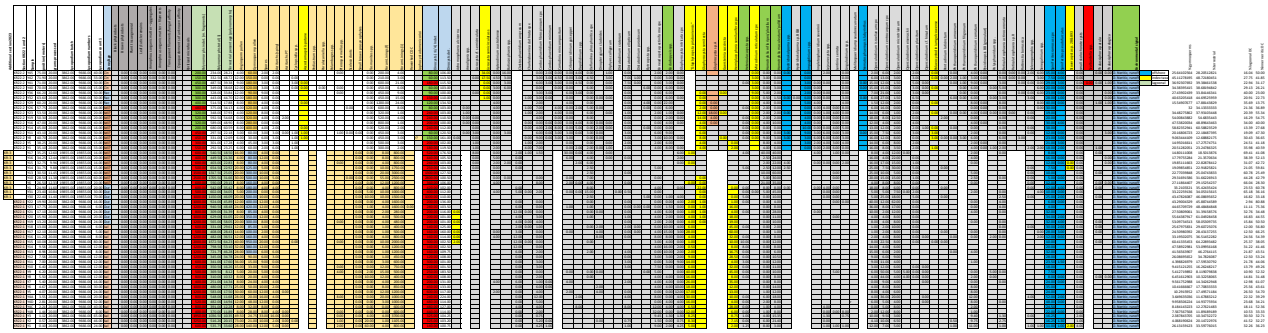

Table S1 The Karaburun composite section dinocyst biostratigraphy chart

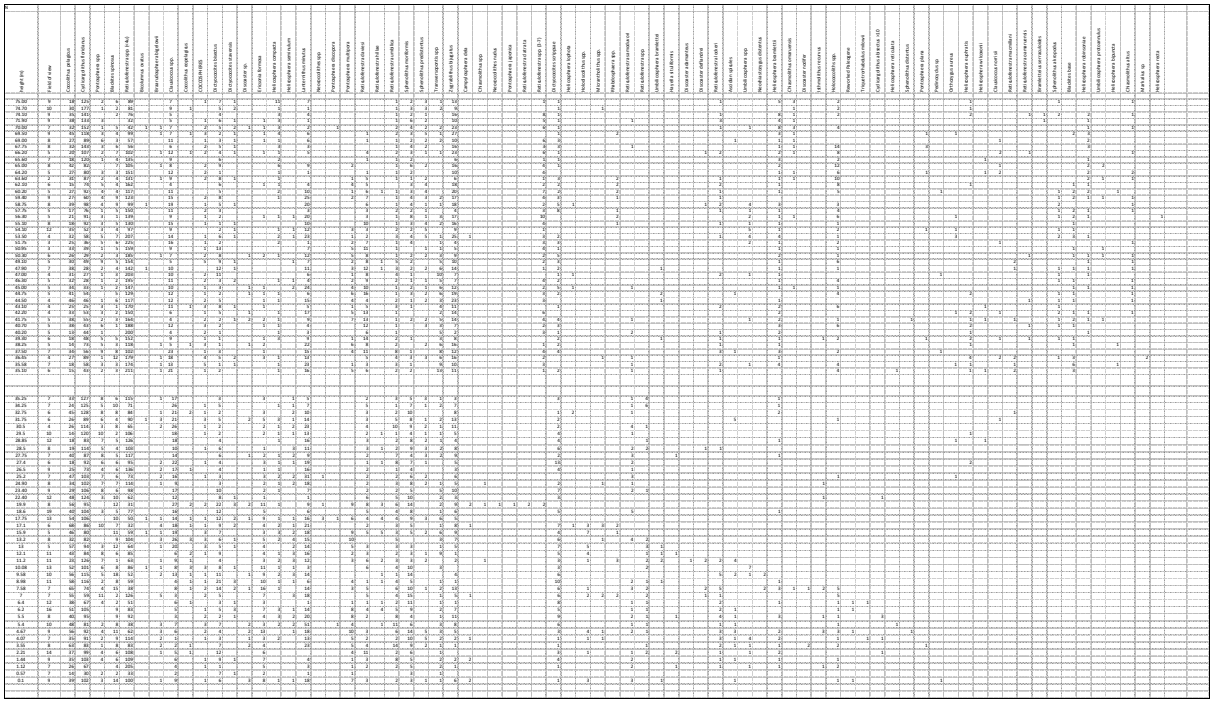

Table S2 The Karaburun composite section calcareous nannofossil biostratigraphy chart

KR2-22						Isotopic Ratios + measurement Uncertainty (2s)									Ages uncorrected for common lead + measurement Uncertainty (2s)										
						Data for Tera-Wasserburg plot				Data for Wetherill plot																
Sample	Is rejected ?	% common lead (f206c)	206Pb (mV)	U (ppm)	U/Th	238U/206Pb	238U/206Pb Uncertainty (% 2s)	207Pb/206Pb	207Pb/206Pb Uncertainty (% 2s)	207Pb/235U	207Pb/235U Uncertainty (% 2s)	206Pb/238U	206Pb/238U Uncertainty (% 2s)	ρ	Age 206Pb/238U	Age 206Pb/238U measurement Uncertainty (2s)	Age 207Pb/235U	Age 207Pb/235U measurement Uncertainty (2s)	Age 207Pb/206Pb	Age 207Pb/206Pb measurement Uncertainty (2s)	Discordance 206Pb/238U vs 207Pb/235U (%)	Discordance 206Pb/238U vs 207Pb/206Pb (%)	Distance to Concordia	Best age (Concordia)	Best age measurement Uncertainty (2S)	Best age Systematic Uncertainty (2S)
ZC28	0	0.47	660	978.28	0.33	203.31	2.5	0.0493	8.7	0.0334	9.1	0.0049	2.5	0.272	31.6	0.8	33.4	3.0	161.2	70.3	5.2	80.4	5.5	31.6	0.8	0.8
ZC37	0	1.12	1276	1608.82	0.33	200.97	2.0	0.0449	8.4	0.0308	8.6	0.0050	2.0	0.233	32.0	0.6	30.8	2.6	0.0	50.9	-3.9	151.1	-3.9	32.0	0.6	0.7
ZC27	0	0.35	1645	2003.42	0.12	199.81	2.5	0.0511	8.9	0.0353	9.2	0.0050	2.5	0.271	32.2	0.8	35.2	3.2	246.2	39.6	8.6	86.9	9.2	32.2	0.8	0.9
ZC7	0	0.90	1266	1564.49	0.31	198.87	2.6	0.0450	8.3	0.0312	8.7	0.0050	2.6	0.295	32.3	0.8	31.2	2.7	0.0	54.3	-3.6	159.2	-3.6	32.3	0.8	0.9
ZC6	0	0.84	1074	1329.80	0.37	198.01	2.8	0.0458	8.5	0.0319	9.0	0.0051	2.8	0.311	32.5	0.9	31.9	2.8	0.0	86.2	-1.9	361.3	-1.9	32.5	0.9	1.0
ZC11	0	0.48	1462	1826.41	0.19	197.87	2.1	0.0478	8.4	0.0333	8.7	0.0051	2.1	0.238	32.5	0.7	33.3	2.8	88.9	291.3	2.3	63.4	2.4	32.5	0.7	0.7
ZC10	0	0.31	1335	1649.41	0.27	197.25	3.3	0.0503	8.4	0.0352	9.0	0.0051	3.3	0.364	32.6	1.1	35.1	3.1	208.6	48.0	7.1	84.4	7.5	32.6	1.1	1.1
ZC38	0	0.58	2156	2626.23	0.26	195.32	3.3	0.0491	8.1	0.0346	8.8	0.0051	3.3	0.373	32.9	1.1	34.6	3.0	151.8	77.9	4.8	78.3	5.0	32.9	1.1	1.1
ZC33	0	0.20	841	1131.86	0.38	194.07	2.5	0.0514	9.0	0.0365	9.3	0.0052	2.5	0.264	33.1	0.8	36.4	3.3	259.5	39.0	9.1	87.2	9.7	33.1	0.8	0.9
ZC32	0	0.35	790	1017.53	0.37	193.39	2.4	0.0496	9.0	0.0354	9.3	0.0052	2.4	0.254	33.2	0.8	35.3	3.2	176.9	67.6	5.8	81.2	6.1	33.2	0.8	0.9
ZC18	0	0.23	1202	1477.13	0.32	183.01	3.1	0.0496	8.4	0.0374	9.0	0.0055	3.1	0.342	35.1	1.1	37.2	3.3	175.7	70.5	5.7	80.0	6.0	35.1	1.1	1.1
ZC25	0	1.10	1607	1186.51	0.38	121.36	6.3	0.0493	8.4	0.0559	10.5	0.0082	6.3	0.604	52.9	3.3	55.3	5.6	159.5	212.8	4.3	66.8	4.6	52.9	3.3	3.4
ZC1	0	1.22	1062	797.29	0.54	186.21	3.0	0.0789	14.0	0.0584	14.4	0.0054	3.0	0.211	34.5	1.0	57.7	8.0	1169.7	12.5	40.1	97.0	53.2	Discordant	Discordant	Discordant
ZC2	0	3.91	268	353.58	0.26	200.55	3.6	0.0202	10.9	0.0139	11.5	0.0050	3.6	0.311	32.1	1.1	14.0	1.6	0.0	2.7	-129.0	101.2	-68.6	Discordant	Discordant	Discordant
ZC4	0	2.53	410	536.36	0.34	191.35	3.0	0.0317	9.3	0.0228	9.7	0.0052	3.0	0.304	33.6	1.0	22.9	2.2	0.0	6.5	-46.7	103.4	-36.5	Discordant	Discordant	Discordant
ZC5	0	4.25	386	510.65	0.23	203.54	3.6	0.0178	10.0	0.0120	10.7	0.0049	3.6	0.338	31.6	1.1	12.1	1.3	0.0	2.0	-160.1	101.0	-72.9	Discordant	Discordant	Discordant
ZC8	0	3.97	354	436.71	0.35	190.91	3.7	0.0209	9.7	0.0151	10.4	0.0052	3.7	0.352	33.7	1.2	15.2	1.6	0.0	2.7	-121.6	101.4	-63.6	Discordant	Discordant	Discordant
ZC9	0	2.00	1009	1239.66	0.30	197.20	3.4	0.0370	9.5	0.0258	10.0	0.0051	3.4	0.339	32.6	1.1	25.9	2.6	0.0	11.3	-25.8	105.8	-22.4	Discordant	Discordant	Discordant
ZC12	0	1.24	1465	1753.64	0.18	199.93	2.1	0.0424	8.5	0.0292	8.8	0.0050	2.1	0.235	32.2	0.7	29.2	2.5	0.0	24.3	-10.0	115.7	-9.6	Discordant	Discordant	Discordant
ZC14	0	0.95	1171	1213.78	0.32	198.20	2.3	0.0645	10.1	0.0448	10.4	0.0050	2.3	0.220	32.4	0.7	44.5	4.5	756.3	12.7	27.1	95.7	32.6	Discordant	Discordant	Discordant
ZC15	0	1.73	1039	1238.21	0.35	198.07	2.4	0.0380	8.6	0.0264	8.9	0.0050	2.4	0.271	32.5	0.8	26.5	2.3	0.0	11.7	-22.5	106.7	-20.2	Discordant	Discordant	Discordant
ZC16	0	3.76	1270	1531.88	0.22	204.46	2.2	0.0199	8.9	0.0134	9.1	0.0049	2.2	0.238	31.5	0.7	13.5	1.2	0.0	2.1	-132.7	101.2	-75.4	Discordant	Discordant	Discordant
ZC17	0	2.16	820	569.74	0.25	189.84	4.0	0.0841	20.8	0.0611	21.2	0.0053	4.0	0.190	33.9	1.4	60.2	12.4	1294.6	16.6	43.7	97.4	59.6	Discordant	Discordant	Discordant
ZC20	0	6.11	12185	1656.29	0.22	148.02	45.5	0.2978	60.9	0.2773	76.0	0.0068	45.5	0.598	43.4	19.7	248.5	169.1	3458.3	32.8	82.5	98.7	221.2	Discordant	Discordant	Discordant
ZC21	0	2.52	1004	1157.00	0.19	203.08	3.5	0.0321	9.4	0.0218	10.1	0.0049	3.5	0.344	31.7	1.1	21.9	2.2	0.0	6.5	-44.5	103.3	-34.6	Discordant	Discordant	Discordant
ZC22	0	2.80	958	1216.71	0.46	204.92	2.3	0.0303	8.8	0.0204	9.1	0.0049	2.3	0.247	31.4	0.7	20.5	1.8	0.0	5.1	-53.4	102.8	-41.4	Discordant	Discordant	Discordant
ZC23	0	0.98	1235	1055.56	0.46	198.68	4.4	0.0724	15.3	0.0502	15.9	0.0050	4.4	0.276	32.4	1.4	49.7	7.7	995.9	14.8	34.9	96.8	44.9	Discordant	Discordant	Discordant
ZC26	0	1.20	961	1233.65	0.38	202.03	2.4	0.0434	8.9	0.0296	9.2	0.0049	2.4	0.262	31.8	0.8	29.6	2.7	0.0	31.9	-7.6	121.4	-7.3	Discordant	Discordant	Discordant
ZC29	0	0.40	1504	1718.47	0.26	197.34	2.8	0.0540	8.7	0.0377	9.1	0.0051	2.8	0.305	32.6	0.9	37.6	3.4	371.9	23.5	13.4	91.2	14.8	Discordant	Discordant	Discordant
ZC31	0	2.07	808	1108.78	0.52	200.01	2.5	0.0361	9.0	0.0249	9.4	0.0050	2.5	0.271	32.2	0.8	25.0	2.3	0.0	9.6	-28.8	105.2	-25.0	Discordant	Discordant	Discordant
ZC34	0	0.11	1952	2531.41	0.31	205.99	1.6	0.0527	8.4	0.0353	8.5	0.0049	1.6	0.191	31.2	0.5	35.2	2.9	316.9	25.9	11.4	90.2	12.3	Discordant	Discordant	Discordant
ZC35	0	1.42	3390	2131.62	0.11	185.83	3.8	0.0871	10.7	0.0646	11.4	0.0054	3.8	0.337	34.6	1.3	63.5	7.0	1360.8	8.4	45.5	97.5	65.0	Discordant	Discordant	Discordant
ZC36	0	3.36	726	959.32	0.43	204.82	2.2	0.0238	9.0	0.0160	9.3	0.0049	2.2	0.233	31.4	0.7	16.1	1.5	0.0	3.0	-94.6	101.6	-62.2	Discordant	Discordant	Discordant
ZC39	0	2.15	1771	2323.64	0.36	205.38	1.6	0.0341	8.1	0.0229	8.2	0.0049	1.6	0.189	31.3	0.5	23.0	1.9	0.0	6.7	-36.2	104.0	-30.8	Discordant	Discordant	Discordant
ZC40	0	0.20	1906	2431.93	0.29	201.99	1.5	0.0521	8.3	0.0356	8.4	0.0050	1.5	0.174	31.8	0.5	35.5	2.9	290.2	29.5	10.3	89.0	11.1	Discordant	Discordant	Discordant

Table S3 U-Pb data for the 35 analyzed zircon grains